



Interaction between the electric and concentration fields in the fractionation of two macromolecules using a Hybrid Membrane Cell – CFD study

Sónia Isabel Silva Pinto, João Mário Miranda*, João Bernardo Lares Moreira de Campos

*Centro de Estudos de Fenómenos de Transporte, Departamento de Engenharia Química, Faculdade de Engenharia da Universidade do Porto, Rua Dr. Roberto Frias, 4200-465 Porto Portugal
Tel. +351 917933708; Fax: +351 225081692; email: jmiranda@fe.up.pt*

Received 16 November 2010; Accepted 11 April 2011

ABSTRACT

The numerical study of membrane separation processes with electric interactions requires the simultaneous solution of Poisson-Boltzmann, Navier-Stokes and Nernst-Planck equations. A numerical method was developed, and implemented, to deal with the coupling between the electric field, the flow field and the concentration fields of the ionic species in solution. The numerical method was validated supposing limit conditions: a-for a binary ionic solution, the results are similar to those obtained with a simplified method which assumes the Boltzmann distribution of the ionic species; b-for high molecular diffusivity of the components, the convection is negligible, relatively to the diffusion, and the numerical solution is similar to the one obtained for a stagnant fluid. The numerical code developed was applied to study macromolecules fractionation in a hybrid membrane cell (HMC) composed by negatively charged semi-permeable membranes (impermeable to the solutes and permeable to the solvent) and neutral fully-permeable membranes, alternating in series. The normalized concentration profiles of the species along the normal and tangential directions were obtained, as well as the non-dimensional electric potential along the normal direction. When the charge of the semipermeable membrane is identical to the charge of the component with the highest diffusivity, this component moves away from the membrane and the other, with the lowest diffusivity, approaches the membrane. However, due to the interactions between electric and concentration fields, in the region crossed by the streamlines of the concentrate stream, the separation in the fully permeable membranes is worsened.

Keywords: Numerical methods; Electrically charged membranes; Membrane separation processes; Poisson-Boltzmann equation; Nernst-Planck equation; Navier-Stokes equation; Hybrid Membrane Cell

1. Introduction

The authors of the present paper have been exploring the potential of different types of hybrid membrane cells (HMC) to fractionate macromolecules [1,2]. Generically, an HMC is composed by two kinds of membranes

alternating in series: a semi-permeable membrane and a fully-permeable membrane [1,2].

The first study was about a HMC with a semi-permeable membrane only permeable to the solvent, and a fully-permeable membrane permeable to both solutes and solvent [1]. The macromolecules separation is done by differential diffusivity. The solute with lower diffusivity remains concentrated near the semi-permeable

*Corresponding author.

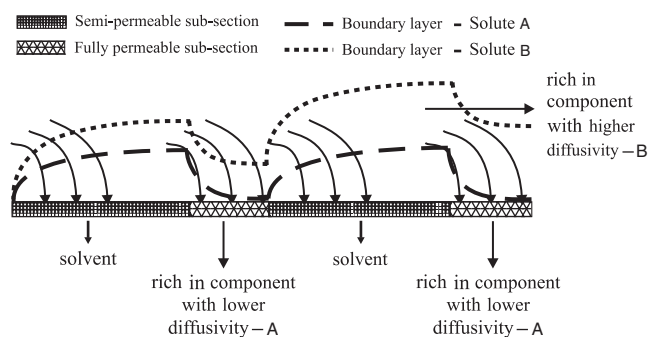


Fig. 1. Differential diffusivity in a Hybrid Membrane Cell.

surface while the solute with higher diffusivity leaves the membrane surface into the bulk. The solute with lower diffusivity, accumulated at the semi-permeable surface, is, preferentially, recovered at the fully-permeable membrane. Therefore, the outflow stream of the cell is rich in the solute with higher diffusivity (Fig. 1) [1].

The second study was about a HMC in which both solutes are transmitted through the semi-permeable membrane, depending on their macromolecules sizes [2]. In this type of HMC, the macromolecules with a size lower than the size of the pores cross preferentially the semi-permeable membrane. The permeate stream leaving this section is then rich in these macromolecules. The solute with macromolecules higher than the size of the pores is retained and leaves the cell, preferentially, through the fully-permeable membranes. This solute has also the lower molecular diffusivity, remaining close to the semi-permeable membranes, a factor that increases the efficiency of the separation.

However, the potential of a HMC can be further explored. Electrical effects were not taken into account in previous works. The careful selection of the charge of the membranes could contribute to optimize the performance of the cells. Further work is needed to understand the influence of the electrical effects on the separation.

The electrical interactions between the membrane and the charged components in the polarized boundary layer are usually neglected in most of the studies. Some attempts have been made to include them in analytical and numerical studies [3–8]. Analytical studies of mass transport in the polarized boundary layer are usually based on the stagnant film model and are not suitable for complex problems involving concentration dependent properties, solutions containing multiple ionic species and membranes with non-uniform zeta potentials. Numerical methods have been applied to the transport in pores or to stagnant boundary layers [8–10]. Related electrochemical problems have been studied in other areas of research, namely electroosmotic flows [11–16]. However, these systems do not combine, as membrane separation processes do, electrochemical transport with tangential and normal convection and concentration polarization.

To study the electric interactions between membrane and components, the Poisson-Boltzmann, the Navier-Stokes and the Nernst-Planck equations need to be solved. In a previous work, these set of equations were solved by a simplified approach [17]. A binary ionic solution was considered and the effect of convection on the ionic distribution was neglected. This simplification removed the coupling between the Poisson-Boltzmann and the Nernst-Planck equations, and the electric potential was determined in a simplified way from the Boltzmann distribution of the charged ions. Moreover, the electric terms of the Navier-Stokes equations were also neglected [17]. However, in practice, most systems have a large number of ionic species and the tangential velocity near the membrane has an important contribution to the mass transport in the cell.

In the present study, the Poisson-Boltzmann, the Navier-Stokes and the Nernst-Planck equations were solved without any simplification. A numerical method was developed to deal with the coupling between the electric and concentration fields of all the species in solution. Both mass transport equations and flow equations have the electric terms incorporated.

The new numerical code developed will be applied to the fractionation of two macromolecules with opposite charges in an ionic solution of NaCl, using a HMC composed by negatively charged semi-permeable membranes (only permeable to the solvent) and neutral fully-permeable membranes (permeable to all components and to the solvent), alternating in series. Additionally to the diffusion mechanisms, already studied by Pinto et al. [1], the importance of the electric interactions in this type of separation is analyzed in this work.

2. Cell description

The HMC under studied is composed by n membrane sections, where each membrane section has a semi-permeable membrane with a zeta potential, Φ_w^s , only permeable to the solvent, and a neutral fully-permeable membrane, permeable to all components (Fig. 2).

In the separation process, the feed stream is separated into three streams: the retentate stream, which leaves the cell through the principal channel, the permeate stream (solvent stream) and the concentrate stream. The solvent is the only component crossing the semi-permeable sub-sections. All the species in solution leave the cell through the neutral fully-permeable sub-sections, which are permeable to all components and to the solvent (concentrate stream).

The characteristics of the conventional cell (CC), with only one semi-permeable membrane, and the characteristics of the HMC, both used in this study, are listed in Table 1. The operational conditions are also presented in this table.

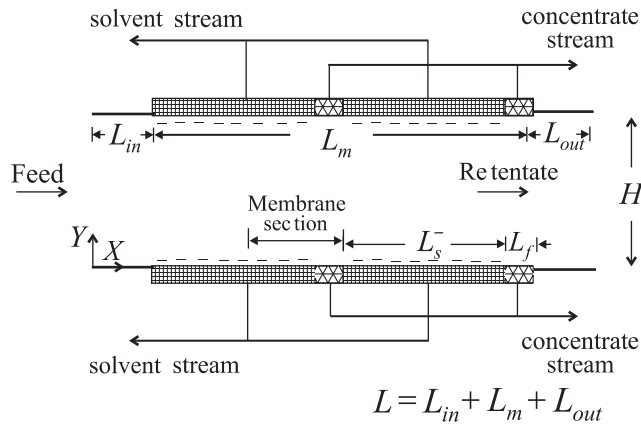


Fig. 2. HMC composed of negatively charged semi-permeable membranes and neutral fully permeable membranes.

Table 1
Characteristics of the conventional cell (CC) and hybrid membrane cell (HMC)

Membrane	CC OMEGA Polysulfone membrane	HMC OMEGA Polysulfone membrane
R_m	$5.714 \times 10^{12} \text{ m}^{-1}$	$5.714 \times 10^{12} \text{ m}^{-1}$
H	0.001 m	0.001 m
L_m	0.250 m	0.2778 m
L_s^-	0.250 m	0.125 m
L_f	–	0.0139 m
ε_f^a	–	10%
n_{sec}	1	2
$\sum_{k=1}^n L_{s,k}^-$	0.250 m	0.250 m
$\sum_{k=1}^n L_{f,k}$	–	0.0278 m
$L_{\text{in}} = L_{\text{out}}$	0.02 m	0.02 m
ΔP_0	$1 \times 10^4 \text{ Pa}$	$1 \times 10^4 \text{ Pa}$

$$^a \varepsilon_f = \frac{L_f}{L_f + L_s^-} \times 100.$$

3. Characterisation of the inlet feed and general assumptions

Inlet feed:

- A mixture of two macromolecules, M_1 and M_2 , with opposite charges, in an ionic solution of NaCl (Na^+ and Cl^-);
- All the species have the same molar concentration ($C_{M,i}^0$) and the solution is electrically neutral, since the sum of the inlet ionic concentrations of all the species is equal to zero.

Table 2
Properties of the components M_1 and M_2 in an ionic solution of NaCl

Component	M_1	M_2	Na^+	Cl^-
M_i (kg/kmol)	69000	10000	23	35.45
Z_i	+2	-2	+1	-1
Pe_i	1.37×10^6	8.00×10^4	7.14×10^4	4.68×10^4
Re	100	100	100	100
C_i^0 (kg/m^3)	6.9×10^{-5}	1.0×10^{-5}	2.30×10^{-8}	3.545×10^{-8}
$C_{M,i}^0$ (kmol/m^3)	1.0×10^{-3}	1.0×10^{-3}	1.0×10^{-3}	1.0×10^{-3}

General assumptions:

- The semi-permeable membrane is considered to be permeable to the solvent but completely impermeable to the solutes;
- The osmotic pressures of the macromolecules, M_1 and M_2 , and of the ionic species, Na^+ and Cl^- , are considered negligible, since the concentrations of these species are, everywhere in the cell including over the semi-permeable membranes, very low (dilute solution);
- The transport properties (viscosity and diffusivity) of all the species are considered constant. In a very diluted solution, viscosity and diffusivity are practically independent of the concentration of the species, including at the membrane surface [18–20];
- The viscosity of the solution is considered identical to that of pure water everywhere inside the cell (very diluted solution);
- Electric effects inside the membrane are not considered.

The properties of the components used are represented in Table 2.

4. Numerical method

In order to study the effect of the electric interactions, it was necessary to determine the electric, the concentration and the flow fields. The Poisson-Boltzmann, the Nernst-Planck and the Navier-Stokes equations were then solved by numerical methods (CFD).

4.1. Domain

The equations were solved in the numerical domain represented in Fig. 3; Fig. 3a) shows the domain of a conventional cell with a semi-permeable membrane; and Fig. 3b) the domain of the HMC represented in Fig. 2. Since the cell is symmetric, the numerical domain encloses half of the cell and comprises an inlet section, an outlet section and the membrane sub-sections.

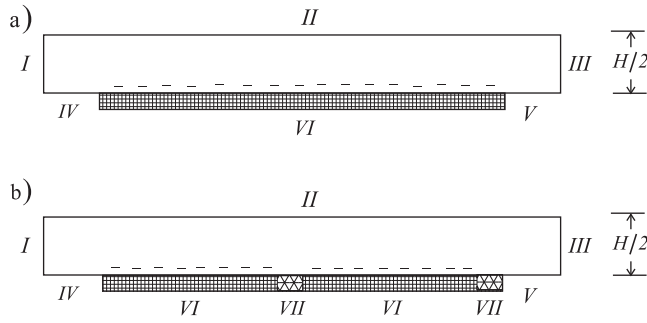


Fig. 3. Schematic representation of the domain: a) conventional cell (CC) b) hybrid membrane cell (HMC) and respective boundaries (I – cell inlet; II – symmetric axis; III – cell outlet; IV – wall; V – wall; VI – semi-permeable membrane with negative zeta-potential; VII – fully-permeable membrane with zeta-potential equal to zero).

4.2. Conservative equations

For a better understanding, from now on, all the lowercase variables symbolize normalized variables: the non-dimensional electric potential is normalized by the absolute value of the semi-permeable membrane potential (Φ_w), the concentrations by the inlet concentrations of the solutes, the velocities by the inlet velocity and the geometric dimensions by the height of the cell. The uppercase variables symbolize dimensional variables.

4.2.1. Electric potential equation

Assuming that the ions in solution can be considered point charges, the electric potential follows the Poisson-Boltzmann equation:

$$\frac{\partial \varphi}{\partial t} = \left(\frac{\partial^2 \varphi}{\partial x^2} + \frac{\partial^2 \varphi}{\partial y^2} \right) + \Pi_2 r_e \quad (1)$$

where φ is the normalized electric potential, r_e the sum of the ionic concentrations of all the components and Π_2 a non-dimensional number defined by:

$$\Pi_2 = \frac{FC_{\text{ref}}^0 H^2}{\epsilon M_{\text{ref}} \Phi_w} \quad (2)$$

where F is the Faraday constant, C_{ref}^0 the concentration of the reference component in the bulk, M_{ref} the molar mass of the reference component and ϵ the permittivity. The cation of the solution, Na^+ , was arbitrarily chosen as the reference component:

$$C_{\text{ref}}^0 = C_{\text{Na}^+}^0 \quad (3)$$

$$M_{\text{ref}} = M_{\text{Na}^+} \quad (4)$$

The sum of the normalized ionic concentrations was determined according to the local ionic concentrations:

$$r_e = \sum_{i=1}^N z_i \frac{C_i^0}{C_{\text{ref}}^0} \frac{M_{\text{ref}}}{M_i} c_i \quad (5)$$

where z_i is the electric charge, c_i the normalized concentration of the component i and M_i the molar mass of component i .

The electric potential Eq. (1) was solved by a fractional-step method with the diffusive terms separated from the independent term. Firstly, the independent term was solved by direct integration. In a second step, the diffusive terms of the electric potential equation were discretized through a finite difference method. The second derivatives were approximated by central differences and the discretized equations were solved by an implicit method.

The boundary conditions of the domain to solve the electric potential equation are listed below:

- At the surface of the semi-permeable and fully-permeable membranes ($y = 0$), the non-dimensional electric potential is equal to the ratio between the potential at the membrane surface and the potential (absolute value) of the semi-permeable membrane:

$$\varphi = \frac{\Phi(y=0)}{\Phi_w} \quad (6)$$

- At the axis of symmetry, the non-dimensional electric potential is equal to zero:

$$\varphi = 0 \quad (7)$$

- At the cell inlet and at the cell outlet, the non-dimensional electric potential is also equal to zero:

$$\varphi = 0 \quad (8)$$

- At the wall of the cell (impermeable areas), the variation of the non-dimensional electric potential along the normal direction is equal to zero:

$$\frac{\partial \varphi}{\partial y} = 0 \quad (9)$$

4.2.2. Flow equations

The flow in the cell is described by the Navier-Stokes and mass conservation equations for a fluid subjected to an electric field [21]:

$$\frac{\partial v_x}{\partial t} + v_x \frac{\partial v_x}{\partial x} + v_y \frac{\partial v_x}{\partial y} = -Eu_0 \frac{\partial p}{\partial x} + \frac{1}{Re} \left(\frac{\partial^2 v_x}{\partial x^2} + \frac{\partial^2 v_x}{\partial y^2} \right) - \Pi_1 r_e \frac{\partial \phi}{\partial x} \quad (10)$$

$$\frac{\partial v_y}{\partial t} + v_x \frac{\partial v_y}{\partial x} + v_y \frac{\partial v_y}{\partial y} = -Eu_0 \frac{\partial p}{\partial y} + \frac{1}{Re} \left(\frac{\partial^2 v_y}{\partial x^2} + \frac{\partial^2 v_y}{\partial y^2} \right) - \Pi_1 r_e \frac{\partial \phi}{\partial y} \quad (11)$$

$$\frac{\partial v_x}{\partial x} + \frac{\partial v_y}{\partial y} = 0 \quad (12)$$

where Π_1 is a non - dimensional number given by:

$$\Pi_1 = \frac{FC_{ref}^0 \Phi_w}{M_{ref} \rho V_0^2} \quad (13)$$

ρ is the fluid density and V_0 the feed velocity. The Reynolds number (Re), based on the height of the parallel plate cell (H) and on the viscosity of the solution ($\bar{\mu}$) is given by:

$$Re = \frac{\rho V_0 H}{\bar{\mu}} \quad (14)$$

The nondimensional number Eu_0 is the Euler number:

$$Eu_0 = \frac{P_0}{\rho V_0^2} \quad (15)$$

where P_0 is the feed pressure.

The Navier-Stokes and the mass conservation equations can also be written for secondary variables (vorticity, ω , and stream function, ψ). For these variables, the equations take the form of the vorticity transport equation:

$$\frac{\partial \omega}{\partial t} + v_x \frac{\partial \omega}{\partial x} + v_y \frac{\partial \omega}{\partial y} = \frac{1}{Re} \left(\frac{\partial^2 \omega}{\partial x^2} + \frac{\partial^2 \omega}{\partial y^2} \right) - \Pi_1 \left(\frac{\partial r_e}{\partial y} \frac{\partial \phi}{\partial x} - \frac{\partial r_e}{\partial x} \frac{\partial \phi}{\partial y} \right) \quad (16)$$

and of a Poisson equation for the stream function:

$$\omega = \frac{\partial^2 \psi}{\partial x^2} + \frac{\partial^2 \psi}{\partial y^2} \quad (17)$$

The vorticity transport equation is obtained by differentiating Eq. (10) in order to y and Eq. (11) in order to x , and subtracting member by member the resulting

equations. The term $-\Pi_1 \left(\frac{\partial r_e}{\partial y} \frac{\partial \phi}{\partial x} - \frac{\partial r_e}{\partial x} \frac{\partial \phi}{\partial y} \right)$ of the vorticity transport equation accounts for the vorticity generation due to the momentum induced by the electric field. The Poisson equation results from the definition of vorticity:

$$\omega = \frac{\partial v_x}{\partial y} - \frac{\partial v_y}{\partial x} \quad (18)$$

and from the definition of stream function:

$$v_x = \frac{\partial \psi}{\partial y}; v_y = -\frac{\partial \psi}{\partial x} \quad (19)$$

The convective, diffusive and independent term (electric term) of the vorticity transport Eq. (16) were discretized by an implicit method. A hybrid method combining upwind and central differences discretizations was used for the convective terms. Central differences discretizations of second order were used for the diffusive terms and for the independent term. The derivatives of Eq. (17) were approximated by second order central differences. The boundary conditions to solve the Navier-Stokes equations are presented in detail in reference [1].

4.2.3. Mass transport equations

The mass transport equation, Nernst-Planck equation, of each component is given by:

$$\frac{\partial c_i}{\partial t} + \frac{\partial (\hat{v}_x c_i)}{\partial x} + \frac{\partial (\hat{v}_y c_i)}{\partial y} = \frac{1}{Pe_i} \left(\frac{\partial^2 c_i}{\partial x^2} + \frac{\partial^2 c_i}{\partial y^2} \right) \quad (20)$$

where

$$\hat{v}_x = \left(v_x - \frac{z_i \Pi_3}{Pe_i} \frac{\partial \phi}{\partial x} \right) \quad (21)$$

$$\hat{v}_y = \left(v_y - \frac{z_i \Pi_3}{Pe_i} \frac{\partial \phi}{\partial y} \right) \quad (22)$$

Pe_i is the Peclet number based on the height of the parallel plate cell (H) and on the diffusivity (D_i) of component i :

$$Pe_i = \frac{V_0 H}{D_i} \quad (23)$$

and Π_3 is a non-dimensional number defined by:

$$\Pi_3 = \frac{F\Phi_w}{RT} \tag{24}$$

The terms $\frac{\partial(\hat{v}_x c_i)}{\partial x}$ and $\frac{\partial(\hat{v}_y c_i)}{\partial y}$ are pseudo-convective terms, and, from a numerical point of view, can be treated by the same method used to discretize the convective terms of the vorticity transport equation. In order to simplify the convergence and resolution of the mass transport equation, Eq. (20) was solved by a fractional-step method, with the pseudo-convective terms separated from the diffusive terms [17].

A finite volume method was used to discretize the pseudo-convective and the diffusive terms. To assure mass conservation, the pseudo-convective terms were discretized by the donor-cell upwind method [17]. More details about the discretization and respective boundary conditions can be found in [17].

4.2.4. Iterative method

The iterative method used to solve the discretized equations is schematically represented in Fig. 4. Starting with the initial conditions (electric potential, concentration and velocity), an iterative cycle was performed to solve the mass transport equation, the electric potential equation, the Poisson equation, and the vorticity transport equation. The velocity components were determined from the stream function definition – Eq. (19).

Electric, concentration and flow fields were studied to analyse the convergence of the numerical method. This study was based on the errors in the concentration of the solutes, in the electric potential and in the vorticity of the flow, in a critical node of the cell. This critical node was located near the cell exit, at the end of last negatively charged semi-permeable membrane, where the convergence is very slow.

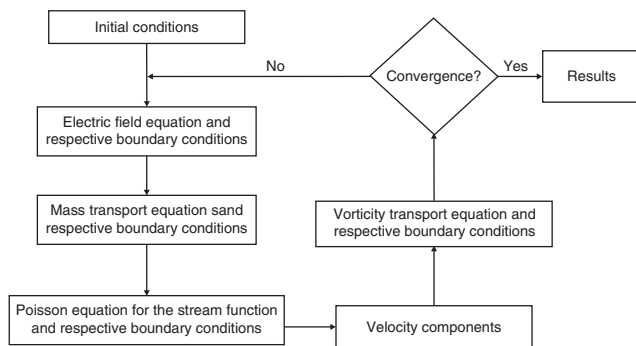


Fig. 4. Flowsheet describing the iterative method to solve the discretized equations.

The error of the concentration of component i in the critical node was determined by:

$$\epsilon_{c_{i,crit}} = \left| \frac{c_{i,crit}^k - c_{i,crit}^{k-1}}{c_{i,crit}^k} \right| \tag{25}$$

The error of the electric potential in the same critical node was determined by:

$$\epsilon_{\phi_{crit}} = \left| \frac{\phi_{crit}^k - \phi_{crit}^{k-1}}{\phi_{crit}^k} \right| \tag{26}$$

and the error of the vorticity in the same critical node was determined by:

$$\epsilon_{\omega_{crit}} = \left| \frac{\omega_{crit}^k - \omega_{crit}^{k-1}}{\omega_{crit}^k} \right| \tag{27}$$

where crit refers to the critical node and k to the current iteration.

Moreover, to assure that the numerical method converges to the correct solution, the total sum of the residues of the electric potential equation, R_ϕ , was determined by:

$$R_\phi = \sum_{g=2}^{n-1} \sum_{h=2}^{m-1} \left| \frac{\partial \phi}{\partial t} \right|_{g,h} \tag{28}$$

where $\left| \frac{\partial \phi}{\partial t} \right|_{g,h}$ is the time derivative of the electric potential at the node (g, h) .

The normalized concentration, the non-dimensional electric potential and the vorticity must converge to a constant value (Fig. 5a and 5b). The total sum of the residues of the electric potential equation dependent on the concentration of the components has to decrease to a very small value (Fig. 5c). The iterative process stops when the following criteria were observed:

$$\begin{cases} \epsilon_{c_{i,crit}} < 10^{-3} \\ \epsilon_{\phi_{crit}} < 10^{-3} \\ \epsilon_{\omega_{crit}} < 10^{-3} \\ R_\phi < 10^{-1} \end{cases} \tag{29}$$

Fig. 5 is an example of the convergence of the numerical data in the separation of M_1 from M_2 , in an ionic solution of NaCl, processed in a hybrid membrane cell with diffusivity and electric mechanisms (most drastic condition used in this paper).

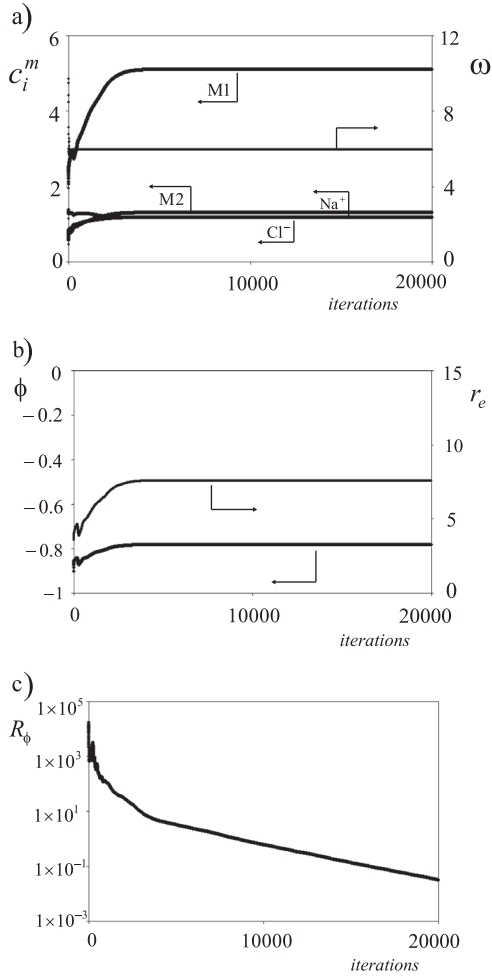


Fig. 5. a) Normalized concentration of the species and vorticity of the flow; b) normalized electric potential and normalized ionic concentration; c) Total residues of the electric potential equation ($C_{M1}^0 = 6.90 \times 10^{-5} \text{ kg/m}^3$, $C_{M2}^0 = 1.00 \times 10^{-5} \text{ kg/m}^3$, $C_{Na^+}^0 = 2.30 \times 10^{-8} \text{ kg/m}^3$, $C_{Cl^-}^0 = 3.545 \times 10^{-8} \text{ kg/m}^3$, $Re = 100$, $Pe_{M1} = 1.30 \times 10^6$, $Pe_{M2} = 8.00 \times 10^4$, $Pe_{Na^+} = 7.14 \times 10^4$, $Pe_{Cl^-} = 4.68 \times 10^4$, $\Pi_1 = 1.07 \times 10^{-4}$, $\Pi_2 = 1.36 \times 10^5$, $\Pi_3 = 0.387$, $\Delta P_0 = 1 \times 10^4 \text{ Pa}$).

4.2.5. Grid optimization

Grid tests were performed to select the best grid. A special care was taken since in a HMC there is an abrupt concentration change in the boundary between semi and fully-permeable membrane sub-sections [1,2]. The independent parameter chosen to perform these tests was the discretization error of the solute concentration expressed by:

$$\epsilon_{C_i^{m,s}} = \frac{\bar{C}_i^{m,s, \text{refgrid}} - \bar{C}_i^{m,s}}{\bar{C}_i^{m,s, \text{refgrid}}} \quad (30)$$

Table 3

Grid tests for the normal direction y ($C_{M1}^0 = 6.90 \times 10^{-5} \text{ kg/m}^3$, $C_{M2}^0 = 1.00 \times 10^{-5} \text{ kg/m}^3$, $C_{Na^+}^0 = 2.30 \times 10^{-8} \text{ kg/m}^3$, $C_{Cl^-}^0 = 3.545 \times 10^{-8} \text{ kg/m}^3$, $Re = 100$, $Pe_{M1} = 1.30 \times 10^6$, $Pe_{M2} = 8.00 \times 10^4$, $Pe_{Na^+} = 7.14 \times 10^4$, $Pe_{Cl^-} = 4.68 \times 10^4$, $\Pi_1 = 1.07 \times 10^{-4}$, $\Pi_2 = 1.36 \times 10^5$, $\Pi_3 = 0.387$, $\Delta P_0 = 1 \times 10^4 \text{ Pa}$)

Grid ($n \times m$)	ni_m^b	$\epsilon_{C_{M1}^{m,s}}$	$\epsilon_{C_{M2}^{m,s}}$
149 \times 251	132	0.53%	0.08%
149 \times 501	132	0.12%	0.06%
149 \times 1001	132	Reference grid	Reference grid

^b ni_m is the number of grid nodes along the total length of the membrane.

Table 4

Grid tests for the tangential direction x ($C_{M1}^0 = 6.90 \times 10^{-5} \text{ kg/m}^3$, $C_{M2}^0 = 1.00 \times 10^{-5} \text{ kg/m}^3$, $C_{Na^+}^0 = 2.30 \times 10^{-8} \text{ kg/m}^3$, $C_{Cl^-}^0 = 3.545 \times 10^{-8} \text{ kg/m}^3$, $Re = 100$, $Pe_{M1} = 1.30 \times 10^6$, $Pe_{M2} = 8.00 \times 10^4$, $Pe_{Na^+} = 7.14 \times 10^4$, $Pe_{Cl^-} = 4.68 \times 10^4$, $\Pi_1 = 1.07 \times 10^{-4}$, $\Pi_2 = 1.36 \times 10^5$, $\Pi_3 = 0.387$, $\Delta P_0 = 1 \times 10^4 \text{ Pa}$)

Grid ($n \times m$)	ni_m^c	$\epsilon_{C_{M1}^{m,s}}$	$\epsilon_{C_{M2}^{m,s}}$
85 \times 501	68	0.48 %	0.31%
149 \times 501	132	0.12 %	0.06%
281 \times 501	264	Reference grid	Reference grid

^c ni_m is the number of grid nodes along the total length of the membrane.

where $\bar{C}_i^{m,s}$ refers to the mean normalized concentration of component i at the semi-permeable membrane surface and the superscript refgrid refers to the reference grid. The results of the grid tests are summarized in Tables 3 and 4.

The results (Tables 3 and 4) show that all the grids are sufficiently accurate since the error is less than 1% relatively to the reference grid. The grid of 149 \times 501 was chosen to obtain the numerical results.

4.2.6. Comparison with previous method

The numerical method developed in the present work is an improvement of the work developed by Pinto et al. [17]. In the method developed by Pinto et al., the electric term of the vorticity equation was neglected [17]:

$$-\Pi_1 \left(\frac{\partial r_e}{\partial y} \frac{\partial \phi}{\partial x} - \frac{\partial r_e}{\partial x} \frac{\partial \phi}{\partial y} \right) = 0 \quad (31)$$

The Boltzmann distribution of ionic species:

$$c_i = c_i^0 \exp[-z_i \Pi_3 (\phi - \phi_0)] \quad (32)$$

was used to determine r_e . In this way, the equation of the electrical potential becomes independent of the concentration field:

$$\frac{\partial \phi}{\partial t} = \left(\frac{\partial^2 \phi}{\partial x^2} + \frac{\partial^2 \phi}{\partial y^2} \right) - 2\Pi_2 \sinh[\Pi_3(\phi - \phi_0)] \quad (33)$$

The electric potential was determined by solving Eq. (33). This step was followed by an iterative method to solve the flow and mass transport equations.

5. Results and discussion

In the work of Pinto et al., the electric field was considered independent of the concentration fields and the electric term of the vorticity equation was neglected [17]. In the present work, the electric field and the concentration fields interact and the electric term of the vorticity equation is taken into account. In the following sections, the effect of these modifications on the concentration and electric fields are going to be studied. Afterwards, a study of the mass transport in a hybrid membrane cell with electric effects will be presented.

5.1. Coupling mass and electric fields

The mass transport in a conventional cell with a negatively charged semi-permeable membrane was simulated to study the interaction between mass and electric fields. The feed stream is an ionic solution of NaCl (Na^+ and Cl^-) and the concentration profiles of the ionic species along the direction perpendicular to the membrane (at the end of the semi-permeable membrane) are shown in Fig. 6 (a and b). The concentration profiles obtained by solving the coupled Poisson-Boltzmann and Nernst-Planck equations are similar to those obtained by the method developed by Pinto et al. [17]. Also shown in the figures are the concentration profiles obtained with the Boltzmann distribution (stagnant liquid conditions). Due to the total rejection of the solutes by the semi-permeable membrane, the concentration values obtained for the permeable system are much higher than those given by Boltzmann distribution.

A maximum is observed in the Cl^- concentration (Fig. 6b). Near the membrane, the solvent is depleted of Cl^- because this ion is repelled by the membrane. Nevertheless, Cl^- accumulates in the boundary layer due to the convective transport. The maximum results from the balance between this transport and the electrical repulsion by the membrane.

The concentration profiles in Fig. 6 depend on the Peclet number (Fig. 7). For decreasing Peclet numbers, the concentration profiles converge to those given by Boltzmann distribution. For small Peclet numbers, the

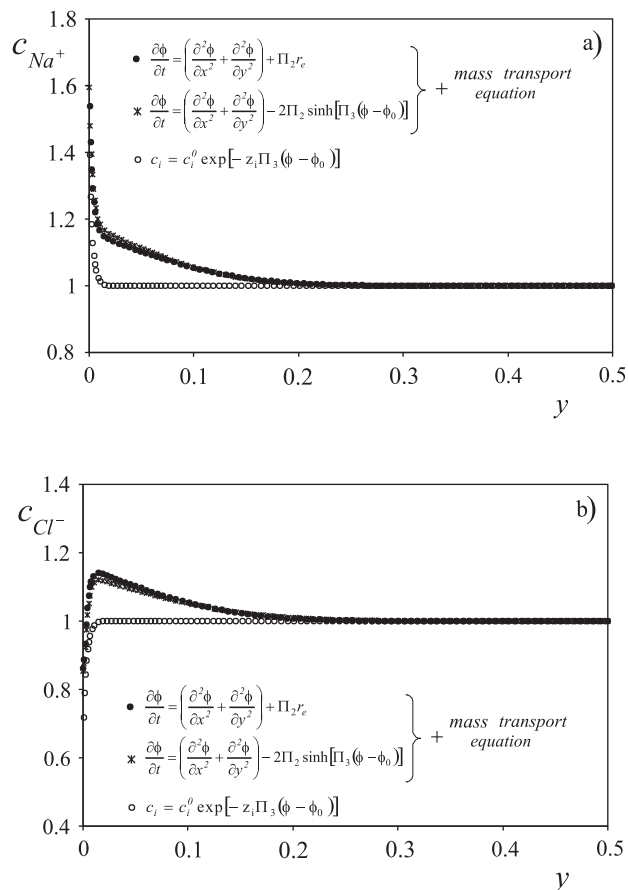


Fig. 6. a) Normalized concentration of Na^+ ; b) Normalized concentration of Cl^- , along the vertical direction, y , at the end of the negatively charged semi-permeable membrane, $x = 260$ ($C_{\text{Na}^+}^0 = 2.30 \times 10^{-8} \text{ kg/m}^3$, $C_{\text{Cl}^-}^0 = 3.545 \times 10^{-8} \text{ kg/m}^3$, $\text{Re} = 100$, $\text{Pe}_{\text{Na}^+} = 7.14 \times 10^4$, $\text{Pe}_{\text{Cl}^-} = 4.68 \times 10^4$, $\Pi_1 = 1.07 \times 10^{-4}$, $\Pi_2 = 1.36 \times 10^5$, $\Pi_3 = 0.387$, $\Delta P_0 = 1 \times 10^4 \text{ Pa}$).

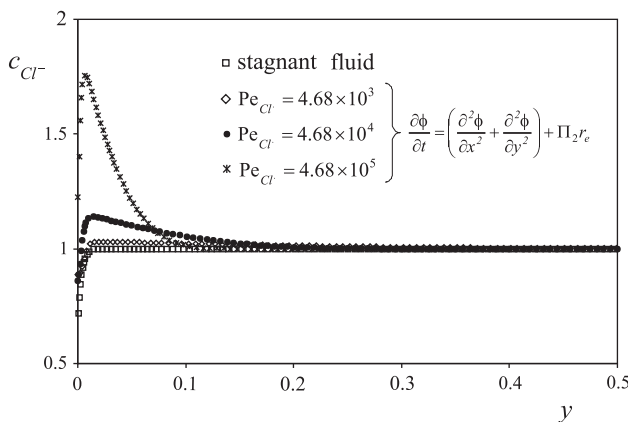


Fig. 7. Normalized concentration of Cl^- along the vertical direction, y , at the end of the negatively charged semi-permeable membrane ($x = 260$), for different Pe_{Cl^-} number: $\text{Pe}_{\text{Cl}^-} = 4.68 \times 10^3$, $\text{Pe}_{\text{Cl}^-} = 4.68 \times 10^4$, and $\text{Pe}_{\text{Cl}^-} = 4.68 \times 10^5$, ($C_{\text{Cl}^-}^0 = 3.545 \times 10^{-8} \text{ kg/m}^3$, $\text{Re} = 100$, $\Pi_1 = 1.07 \times 10^{-4}$, $\Pi_2 = 1.36 \times 10^5$, $\Pi_3 = 0.387$, $\Delta P_0 = 1 \times 10^4 \text{ Pa}$).

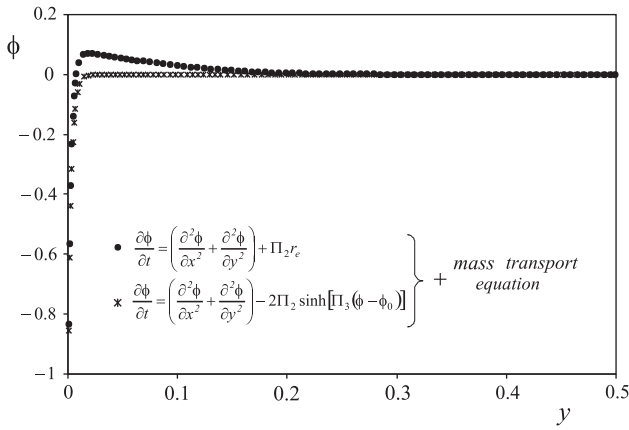


Fig. 8. Non-dimensional electric potential along the vertical direction, y , at the end of the negatively charged semi-permeable membrane, $x = 260$ ($C_{Na^+}^0 = 2.30 \times 10^{-8} \text{ kg/m}^3$, $C_{Cl^-}^0 = 3.545 \times 10^{-8} \text{ kg/m}^3$, $Re = 100$, $Pe_{Na^+} = 7.14 \times 10^4$, $Pe_{Cl^-} = 4.68 \times 10^4$, $\Pi_1 = 1.07 \times 10^{-4}$, $\Pi_2 = 1.36 \times 10^5$, $\Pi_3 = 0.387$, $\Delta P_0 = 1 \times 10^4 \text{ Pa}$).

tangential convection is negligible and the mass transport becomes similar to the mass transport in a stagnant liquid, for which the Boltzmann distribution is accurate.

The electric potential as a function of the normal distance to the membrane is represented in Fig. 8. This figure shows that the electric potential obtained by solving the coupled Poisson-Boltzmann and Nernst-Planck equations is higher than that obtained by solving the Poisson-Boltzmann equation assuming Boltzmann distribution (Pinto et al. [17]). The difference results from the fact that the ionic concentrations are also significantly different. The electric potential has a maximum in a region very close to the membrane surface.

5.2. Coupling electric and flow fields

The separation of two macromolecules, M_1 and M_2 , in an ionic solution of NaCl, was used to study the effect of the electric term of the vorticity equation. A conventional cell with only one negatively charged semi-permeable membrane was simulated. The results are represented in Fig. 9.

Fig. 9 shows that the velocity profiles (Figs. 9a and 9b), obtained by solving the vorticity equation with and without the electric term, are similar. As a consequence, the concentration profiles and the electric field are also unaffected by the electric term (Figs. 9c–9e).

Fig. 9d shows that the concentration fields interact with the potential field leading to the formation of a maximum of the electric field for $y = 0.005$. This maximum attracts the negatively charged ions and repels the positively charged ions. In the case of species with high diffusivity, a pronounced maximum (Cl^-) and a pronounced minimum (Na^+) are observed.

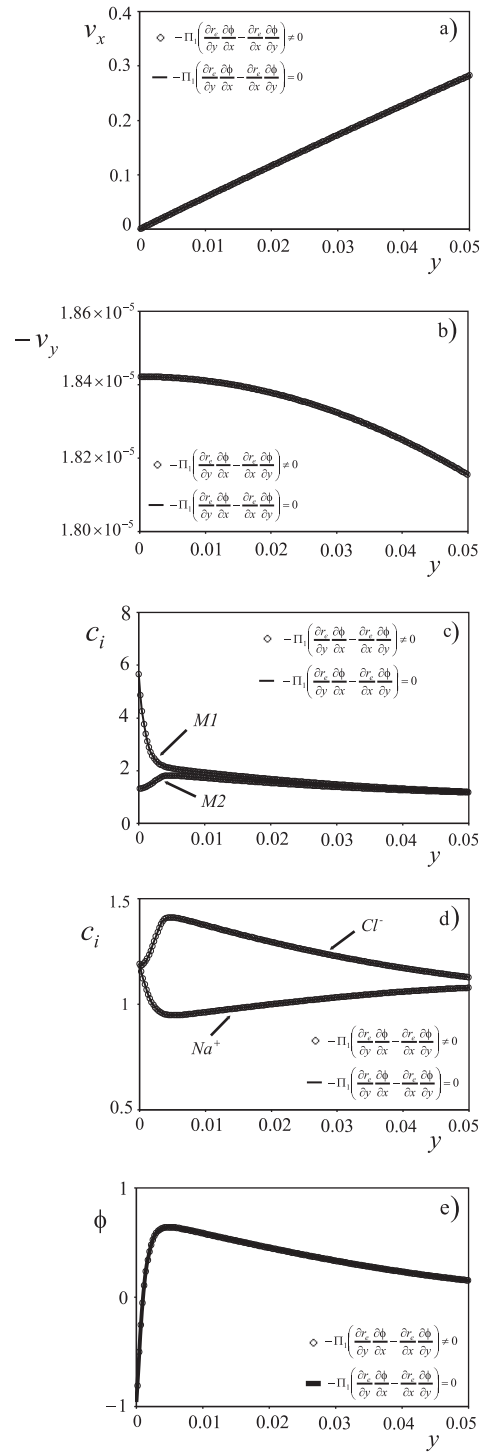


Fig. 9. a) Longitudinal velocity component; b) Normal velocity component; c) Normalized concentration of M_1 and M_2 ; d) Normalized concentration of Na^+ and Cl^- ; e) Non-dimensional electric potential, at the end of the negatively charged semi-permeable membrane, $x = 260$ ($C_{M1}^0 = 6.90 \times 10^{-5} \text{ kg/m}^3$, $C_{M2}^0 = 1.00 \times 10^{-5} \text{ kg/m}^3$, $C_{Na^+}^0 = 2.30 \times 10^{-8} \text{ kg/m}^3$, $C_{Cl^-}^0 = 3.545 \times 10^{-8} \text{ kg/m}^3$, $Re = 100$, $Pe_{M1} = 1.30 \times 10^6$, $Pe_{M2} = 8.00 \times 10^4$, $Pe_{Na^+} = 7.14 \times 10^4$, $Pe_{Cl^-} = 4.68 \times 10^4$, $\Pi_1 = 1.07 \times 10^{-4}$, $\Pi_2 = 1.36 \times 10^5$, $\Pi_3 = 0.387$, $\Delta P_0 = 1 \times 10^4 \text{ Pa}$).

5.3. Fractionation of two macromolecules in a HMC

The fractionation of two macromolecules, M_1 and M_2 , in a HMC was numerically simulated. Fig. 10 compares the concentration of the solutes at the membrane surface for a system with electrically charged semi-permeable membranes ($\Phi_w^s = -0.01$) with data from a system with electrically neutral semi-permeable membranes ($\Phi_w^s = 0$). Fig. 11 is a detailed representation of the concentration profiles at the surface of the second fully-permeable membrane.

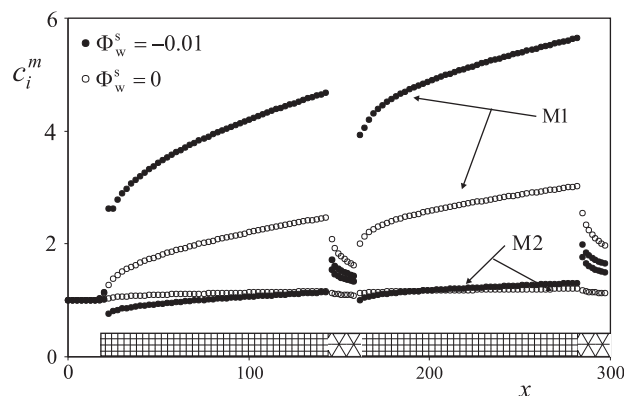


Fig. 10. Normalized concentration profiles of M_1 and M_2 along the tangential direction, x , at the hybrid membrane cell surface ($C_{M1}^0 = 6.90 \times 10^{-5} \text{ kg/m}^3$, $C_{M2}^0 = 1.00 \times 10^{-5} \text{ kg/m}^3$, $C_{\text{Na}^+}^0 = 2.30 \times 10^{-8} \text{ kg/m}^3$, $C_{\text{Cl}^-}^0 = 3.545 \times 10^{-8} \text{ kg/m}^3$, $\text{Re} = 100$, $\text{Pe}_{M1} = 1.30 \times 10^6$, $\text{Pe}_{M2} = 8.00 \times 10^4$, $\text{Pe}_{\text{Na}^+} = 7.14 \times 10^4$, $\text{Pe}_{\text{Cl}^-} = 4.68 \times 10^4$, $\Pi_1 = 1.07 \times 10^{-4}$, $\Pi_2 = 1.36 \times 10^5$, $\Pi_3 = 0.387$, $\Delta P_0 = 1 \times 10^4 \text{ Pa}$).

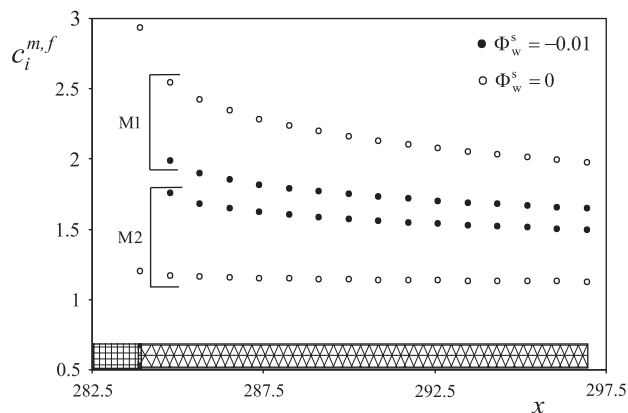
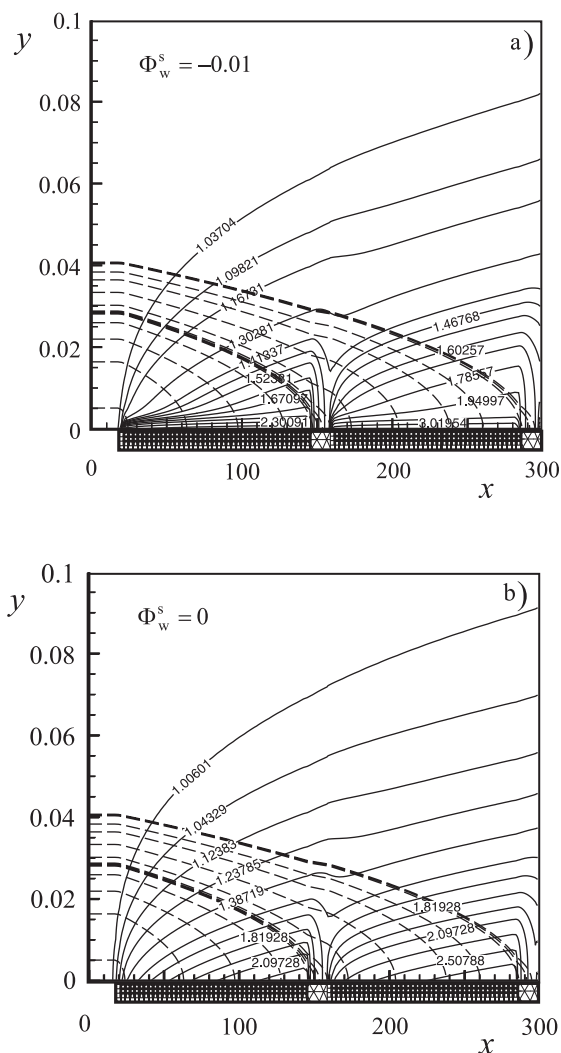


Fig. 11. Normalized concentration profiles of M_1 and M_2 along the last (2nd) fully-permeable sub-section at the hybrid membrane cell surface ($C_{M1}^0 = 6.90 \times 10^{-5} \text{ kg/m}^3$, $C_{M2}^0 = 1.00 \times 10^{-5} \text{ kg/m}^3$, $C_{\text{Na}^+}^0 = 2.30 \times 10^{-8} \text{ kg/m}^3$, $C_{\text{Cl}^-}^0 = 3.545 \times 10^{-8} \text{ kg/m}^3$, $\text{Re} = 100$, $\text{Pe}_{M1} = 1.30 \times 10^6$, $\text{Pe}_{M2} = 8.00 \times 10^4$, $\text{Pe}_{\text{Na}^+} = 7.14 \times 10^4$, $\text{Pe}_{\text{Cl}^-} = 4.68 \times 10^4$, $\Pi_1 = 1.07 \times 10^{-4}$, $\Pi_2 = 1.36 \times 10^5$, $\Pi_3 = 0.387$, $\Delta P_0 = 1 \times 10^4 \text{ Pa}$).

When negatively charged semi-permeable membranes are used:

- the concentration of the positively charged macromolecule (M_1) is higher at the semi-permeable membrane surface and lower at the fully-permeable membrane surface;
- the concentration of the negatively charged macromolecule (M_2) is lower at the surface of the semi-permeable membranes and higher at the surface of the fully-permeable membranes.



At the surface of the semi-permeable membrane, the separation of the components increases because the electrical effects add to the diffusional effects. The component with the lower diffusivity is also the positively charged component and so its concentration over the surface of the semi-permeable membrane increases. The opposite occurs with the negatively charged component: higher diffusivity and electrical repulsion contribute to a low concentration of this component over the semi-permeable membrane.

At the surface of the fully-permeable membranes, the separation of the components decreases. To understand this decrease, the concentration field in the region near the surface of the membranes must be analysed. The concentration fields of the positively charged component in this region are represented in Fig. 12 for $\Phi_w^s = -0.01$ and $\Phi_w^s = 0$.

The concentration at the fully-permeable membranes is a consequence of the transport of solutes along the

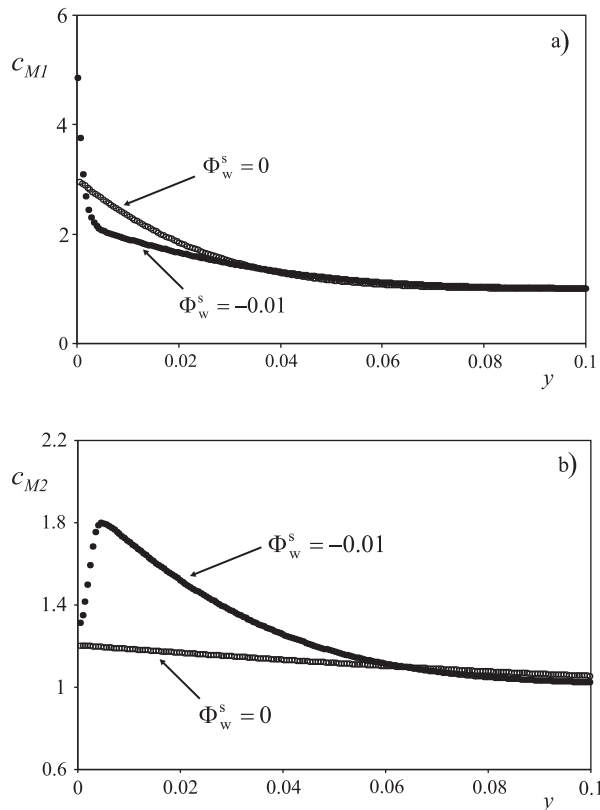


Fig. 13. a) Normalized concentration profile of M_1 ; b) Normalized concentration profile of M_2 , along the vertical direction, y , at the end of the last (2nd) negatively charged semi-permeable membrane, $x = 260$ ($C_{M1}^0 = 6.90 \times 10^{-5} \text{ kg/m}^3$, $C_{M2}^0 = 1.00 \times 10^{-5} \text{ kg/m}^3$, $C_{Na^+}^0 = 2.30 \times 10^{-8} \text{ kg/m}^3$, $C_{Cl^-}^0 = 3.545 \times 10^{-8} \text{ kg/m}^3$, $Re = 100$, $Pe_{M1} = 1.30 \times 10^6$, $Pe_{M2} = 8.00 \times 10^4$, $Pe_{Na^+} = 7.14 \times 10^4$, $Pe_{Cl^-} = 4.68 \times 10^4$, $\Pi_1 = 1.07 \times 10^{-4}$, $\Pi_2 = 1.36 \times 10^5$, $\Pi_3 = 0.387$, $\Delta P_0 = 1 \times 10^4 \text{ Pa}$).

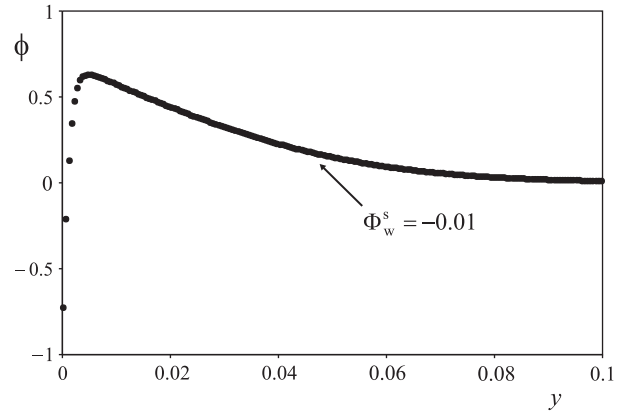


Fig. 14. Non-dimensional electric potential along the vertical direction, y , at the end of the last (2nd) negatively charged semi-permeable membrane, $x = 260$ ($C_{M1}^0 = 6.90 \times 10^{-5} \text{ kg/m}^3$, $C_{M2}^0 = 1.00 \times 10^{-5} \text{ kg/m}^3$, $C_{Na^+}^0 = 2.30 \times 10^{-8} \text{ kg/m}^3$, $C_{Cl^-}^0 = 3.545 \times 10^{-8} \text{ kg/m}^3$, $Re = 100$, $Pe_{M1} = 1.30 \times 10^6$, $Pe_{M2} = 8.00 \times 10^4$, $Pe_{Na^+} = 7.14 \times 10^4$, $Pe_{Cl^-} = 4.68 \times 10^4$, $\Pi_1 = 1.07 \times 10^{-4}$, $\Pi_2 = 1.36 \times 10^5$, $\Pi_3 = 0.387$, $\Delta P_0 = 1 \times 10^4 \text{ Pa}$).

streamlines that cross these sub-sections. The concentration of the positively charged component along these streamlines, in the region slightly above the end of the semi-permeable membranes, is lower for $\Phi_w^s = -0.01$. The reverse phenomenon occurs for the negatively charged component.

Fig. 13 shows the concentration profiles along the vertical direction, y , at the end of the second semi-permeable membrane. In the region crossed by the streamlines of the concentrate stream (around $y = 0.005$), the concentration of M_1 is lower for $\Phi_w^s = -0.01$ than for $\Phi_w^s = 0$ and the concentration of M_2 is higher for $\Phi_w^s = -0.01$ than for $\Phi_w^s = 0$. For $y = 0.005$, the concentration of M_1 has a sudden change in slope and the concentration of M_2 has a maximum. These features of the concentration profiles are related to a maximum in the electric potential (Fig. 14). This maximum, $\phi = 0.6$, repels the positively charged component and attracts the negatively charged one.

6. Conclusions

A new numerical code was developed to simulate the fractionation of macromolecules by membrane cells. The main goal is to extend to multi-component ionic solutions the code developed by Pinto et al. [17] for binary ionic solutions.

The Poisson-Boltzmann, Nernst-Planck and Navier-Stokes equations were solved by numerical methods, without any simplification. The results were compared with those given by a simplified version developed by Pinto et al. [17]. The data from both methods, for a

binary ionic solution, are very similar. If the Peclet number of the components is low (high diffusivity), the convection is negligible relatively to the diffusion. In this case, the solution is similar to that obtained considering stagnant fluid.

A sensitivity analysis of the electric terms of the vorticity equation was also done. The influence of the electric terms of the vorticity equation on the numerical results is negligible.

The new numerical code was applied to the fractionation of two macromolecules using a HMC. The HMC comprised neutral fully permeable membranes and semi-permeable membranes with the charge of the component with higher diffusivity. The numerical results were compared to those in a HMC but supposing semi-permeable membranes electrically neutral. The separation improves in the boundary layer over the semi-permeable membrane. However, the separation in the fully-permeable membranes is lower.

In a future work, the numerical code developed will be applied to the separation of two macromolecules by a hybrid membrane cell but with charged semi-permeable membranes selective to the components, i.e., permeable to the macromolecules, according to the size of macromolecules and to the membrane pore size. In this type of cell, it is expected that electric effects can increase the separation, as long as the most transmitted component through the membrane is also the most electrically attracted to the membrane.

Acknowledgements

The authors gratefully acknowledge the financial support of Fundação para a Ciência e Tecnologia (FCT) through project POCI/EQU/59724/2004 and scholarship SFRH/BD/27821/2006. POCTI (FEDER) also supported this work via CEFT.

Symbols

C_i	— Concentration of component i
c_i	— Normalized concentration of component i
C_i^0	— Concentration of component i at the feed/bulk
c_i^0	— Normalized concentration of component i at the feed/bulk
C_{ref}^0	— Concentration of the reference component at the feed/bulk
c_{ref}^0	— Normalized concentration of the reference component at the feed/bulk
$C_{M,i}^0$	— Molar concentration of component i at the feed/bulk
$c_{M,i}^0$	— Normalized molar concentration of component i at the feed/bulk
C_i^m	— Concentration of component i at membrane surface

c_i^m	— Normalized concentration of component i at membrane surface
$C_i^{m,f}$	— Concentration of component i at fully-permeable membrane surface
$c_i^{m,f}$	— Normalized concentration of component i at fully-permeable membrane surface
$C_{i,\text{crit}}^k$	— Concentration of component i on a critical location
$c_{i,\text{crit}}^k$	— Normalized concentration of component i on a critical location
$\bar{C}_i^{m,s}$	— Mean concentration of component i at semi-permeable membrane surface
$\bar{c}_i^{m,s}$	— Mean normalized concentration of component i at semi-permeable membrane surface
$\bar{C}_i^{m,s,\text{refgrid}}$	— Mean concentration of component i at semi-permeable membrane surface for a reference grid
$\bar{c}_i^{m,s,\text{refgrid}}$	— Mean normalized concentration of component i at semi-permeable membrane surface for a reference grid
D_i	— Molecular diffusivity of component i
F	— Faraday constant
H	— Distance between parallel plates
k	— Current time step
L_{out}	— Length of the outlet section
L_{in}	— Length of the inlet section
L_m	— Total length of the membrane
L_s^-	— Length of the negatively charged semi-permeable sub-section
$\sum_{k=1}^n L_{s,k}^-$	— Total length of the negatively charged semi-permeable membrane
L_f	— Length of the neutral fully-permeable sub-section
$\sum_{k=1}^n L_{f,k}$	— Total length of the neutral fully-permeable membrane
L	— Total length of the cell
M_i	— Molar mass of component i
M_{ref}	— Molar mass of the reference component
m	— Total number of nodes in the vertical direction of the grid
n	— Total number of nodes in the horizontal direction of the grid
ni_m	— Number of nodes along the total length of the membrane
n_{sec}	— Number of sections of the hybrid membrane cell
R	— Gas constant
r_e	— Sum of the normalized ionic concentrations
R_m	— Membrane resistance of the semi-permeable membrane
T	— Temperature
t	— Non-dimensional time
V_0	— Mean feed velocity
V_x	— Longitudinal component of the velocity

v_x	—	Normalized longitudinal component of the velocity
\hat{v}_x	—	Normalized pseudo-velocity (component x)
V_y	—	Vertical component of the velocity
v_y	—	Normalized vertical component of the velocity
\hat{v}_y	—	Normalized pseudo-velocity (component y)
X	—	Longitudinal coordinate
x	—	Normalized longitudinal coordinate
Y	—	Vertical coordinate
y	—	Normalized vertical coordinate
z_i	—	Electric charge of component i

Non-dimensional numbers

Pe_i	—	Peclet number of component i
Re	—	Reynolds number of the solution
Π_1	—	Non-dimensional number defined by equation 13
Π_2	—	Non-dimensional number defined by equation 2
Π_3	—	Non-dimensional number defined by equation 24

Greek Symbols

ΔP_0	—	Static pressure difference across the semi-permeable membrane
Δt	—	Time step range
ε	—	Permittivity
ε_{crit}^i	—	Numerical error of the concentration of component i on a critical location
ε_{crit}	—	Numerical error of the electric potential on a critical location
$\varepsilon_{\omega crit}$	—	Numerical error of the vorticity on a critical location
$\varepsilon_{c_i}^{m,s}$	—	Discretization error of concentration of component i at semi-permeable membrane surface
Ψ	—	Stream function
ω	—	Vorticity
ω_{crit}^k	—	Vorticity on a critical location
ρ	—	Density
$\bar{\mu}$	—	Mean viscosity of the solution
Φ	—	Electric potential
ϕ	—	Normalized electric potential
Φ_0	—	Electric potential of the bulk
ϕ_0	—	Normalized electric potential of the bulk
Φ_w	—	Membrane electric potential
ϕ_w	—	Normalized membrane electric potential
Φ_w^s	—	Electric potential at semi-permeable membrane surface
ϕ_{crit}^k	—	Normalized electric potential on a critical location

References

- [1] S.I.S. Pinto, T.M.G.T. Rocha, J.M. Miranda and J.B.L.M. Campos, A new membrane fractionation process based on the combination of hybrid membrane cells and differential diffusion of two solutes, *Desalination*, 241 (2009) 372–387.
- [2] S.I.S. Pinto, J.M. Miranda and J.B.L.M. Campos, Use of Hybrid Membrane Cells to improve the apparent selectivity in the fractionation of two components – CFD study, *Ind. & Eng. Chem. Res.*, 49 (2010) 9978–9987.
- [3] R. Ghosh and Z.F. Cui, Simulation study of the fractionation of proteins using ultrafiltration, *J. Membr. Sci.*, 180 (2000) 29–36.
- [4] S. De and P.K. Bhattacharya, Mass transfer coefficient with suction including property variations in applications of cross-flow ultrafiltration, *Sep. Purif. Technol.*, 16 (1999) 61–73.
- [5] S.R. Bellara and Z. Cui, A Maxwell-Stefan approach to modelling the cross-flow ultrafiltration of protein solutions in tubular membranes, *Chem. Eng. Sci.*, 53 (1998) 2153–2166.
- [6] S.S. Vasan, R.W. Field and Z. Cui, A Maxwell–Stefan–Gouy–Debye model of the concentration profile of a charged solute in the polarisation layer, *Desalination*, 192 (2006) 356–363.
- [7] M. Rabiller-Baudry, B. Chaufer, P. Aimar, B. Bariou and D. Lucas, Application of a convection–diffusion–electrophoretic migration model to ultrafiltration of lysozyme at different pH values and ionic strengths, *J. Membr. Sci.*, 179 (2000) 163–174.
- [8] V.V. Nikonenko, K.A. Lebedev and S.S. Suleimanov, Influence of the Convective Term in the Nernst–Planck Equation on Properties of Ion Transport through a Layer of Solution or Membrane, *Russ. J. Electrochem.*, 45 (2009) 160–169.
- [9] S. Basu and M.M. Sharma, An improved Space-Charge model for flow through charged microporous membranes, *J. Membr. Sci.*, 124 (1997) 77–91.
- [10] A. Szymczyk, P. Fievet, B. Aoubiza, C. Simon and J. Pagetti, An application of the space charge model to the electrolyte conductivity inside a charged microporous membrane, *J. Membr. Sci.*, 161 (1999) 275–285.
- [11] H.M. Park, J.S. Lee and T.W. Kim, Comparison of the Nernst–Planck model and the Poisson–Boltzmann model for electroosmotic flows in microchannels, *J. Colloid Interface Sci.*, 315 (2007) 731–739.
- [12] Y. Zhang, X.-J. Gu, R.W. Barber and D.R. Emerson, An analysis of induced pressure fields in electroosmotic flows through microchannels, *J. Colloid Interface Sci.* 275 (2004) 670–678.
- [13] W.B. Zimmerman, *Electrochemical microfluidics*, *Chem. Eng. Sci.* (2010), doi:10.1016/j.ces.2010.03.057.
- [14] T.J. Craven, J.M. Rees and W.B. Zimmerman, On slip velocity boundary conditions for electroosmotic flow near sharp corners, *Physics of Fluids*, 20 (2008) 043603.
- [15] L.-M. Fu, J.-Y. Lin, and R.-J. Yang, Analysis of electroosmotic flow with step change in zeta potential, *J. Colloid Interface Sci.* 258 (2003) 266–275.
- [16] J. Alam and J.C. Bowman, Energy-Conserving Simulation of Incompressible Electro-Osmotic and Pressure-Driven Flow, *Theor. Comput. Fluid Dyn.* 16 (2002) 133–150.
- [17] S.I.S. Pinto, J.M. Miranda and J.B.L.M. Campos, Numerical study of the effect of a charged membrane in the separation of electrically charged components, *Desalin. Water Treat.* 14 (2010) 201–207.
- [18] W. Leung and R.F. Probstein, Low polarization in laminar ultrafiltration of macromolecular solutions, *Ind. Eng. Chem. Fundam.*, 18 (1979) 274.
- [19] P. Pivonka, C. Hellmich and D. Smith, Microscopic effects on chloride diffusivity of cement pastes – a scale-transition analysis, *Cem. Concr. Res.*, 34 (2004) 2251–2260.
- [20] W.N. Gill, D.E. Wiley, C.J.D. Fell and A.G. Fane, Effect of viscosity on concentration polarization in ultrafiltration, *AIChE J.* 34 (1988) 1563–1567.
- [21] J.M. MacInnes, Computation of reacting electrokinetic flow in microchannel geometries, *Chem. Eng. Sci.*, 57 (2002) 4539–4558.